1 December 2000

ELSEVIER

Chemical Physics Letters 331 (2000) 170–176

CHEMICAL PHYSICS LETTERS

www.elsevier.nl/locate/cplett

Rate coefficients and cross-sections for the reactions of $C(^3P_J)$ atoms with methylacetylene and allene

Delphine Chastaing [a], Sébastien D. Le Picard [a], Ian R. Sims [a], Ian W.M. Smith [a], Wolf D. Geppert [b], Christian Naulin [b], Michel Costes [b,*]

[a] *School of Chemistry, The University of Birmingham, Edgbaston, Birmingham B15 2TT, UK*

[b] *UMR 5803 CNRS – Université Bordeaux I, Laboratoire de Physico-Chimie Moléculaire, Université Bordeaux I, 33405 Talence Cedex, France*

Received 3 October 2000

Abstract

The reactivity of $C(^3P_J)$ atoms towards methylacetylene and allene has been investigated using complementary experimental methods. Kinetic measurements performed over the range $T = 15$–295 K have yielded thermal rate coefficients: $(2.7 \pm 0.6) \times 10^{-10}(T/298\ \mathrm{K})^{-(0.11\pm0.07)}$ and $(3.5 \pm 0.8) \times 10^{-10}(T/298\ \mathrm{K})^{-(0.01\pm0.12)}$ cm^3 molecule^{-1} s^{-1}, respectively. Crossed beam experiments conducted in the range of relative translational energies $\varepsilon_{tr} = 4.9$–282 meV have yielded integral cross-sections for $H(^2S_{1/2})$ production that are proportional to $(\varepsilon_{tr})^{-0.56\pm0.02}$ and $(\varepsilon_{tr})^{-0.55\pm0.01}$, respectively, in excellent agreement with the temperature dependencies of the rate coefficients.

1. Introduction

Reactions of ground-state atomic carbon $C(^3P_J)$ with unsaturated hydrocarbons have been a subject of increasing interest in recent years. Initially triggered by the kinetic measurements performed by Husain and Haider [1–3], who demonstrated that these reactions are very fast at room temperature, the proposition that they would take place without any activation barrier and would thus remain rapid at very low temperatures has set an interesting challenge [4]. Furthermore, $C(^3P_J)$ has been found to be particularly abundant in dense interstellar clouds (ISCs) where very low temperatures, typically 10–50 K are prevalent [5,6]. The potential importance of $C(^3P_J)$ reactions with unsaturated hydrocarbons has been invoked in the synthesis of large carbon-bearing species in ISCs. Schemes involving successive insertion–elimination reactions of the type $C(^3P_J) + C_nH_m \rightarrow C_{n+1}H_{m-1} + H$ have been proposed by Herbst and coworkers [7,8]. Several such reactions have been investigated by Kaiser et al. [9–11], in crossed molecular beam experiments, performed at relative translational energies corresponding to temperatures between 700 and 3500 K.

Kinetic studies of $C(^3P_J)$ reactions at the very low temperatures (down to 15 K) relevant to ISCs are now possible, thanks to the Cinétique de Réaction en Ecoulement Supersonique Uniforme (CRESU) technique [12]. Rate coefficients for a number of reactions of $C(^3P_J)$, obtained with the

* Corresponding author. Fax: +33-5-56-84-66-45.
E-mail address: costes@cribx1.u-bordeaux.fr (M. Costes).

0009-2614/00/$ - see front matter
PII: S0009-2614(00)01231-8

Birmingham CRESU apparatus, have been reported recently [13–16]. Dynamics studies are also feasible at very low relative translational energies (down to $\varepsilon_{tr} = 4$ meV) with a crossed beam experiment in Bordeaux [15,17]. The present Letter compares new kinetics and dynamics results on the following exoergic reactions of $C(^3P_J)$ with methylacetylene and allene [10,11]:

$$C(^3P_J) + CH_3C{\equiv}CH \rightarrow C_4H_3 + H, \quad \Delta\varepsilon_0 = -2.01 \text{ eV}; \tag{1}$$

$$C(^3P_J) + H_2C{=}C{=}CH_2 \rightarrow C_4H_3 + H, \quad \Delta\varepsilon_0 = -1.87 \text{ eV}. \tag{2}$$

2. Experimental

2.1. Kinetic experiments

The rate coefficients have been measured in the Birmingham CRESU apparatus at six temperatures between 15 and 295 K. An extensive description of this equipment has been given elsewhere [18]. The flow conditions used in the present experiments are listed in Table 1. $C(^3P_J)$ atoms were generated by pulsed laser photolysis of C_3O_2 at 193 nm and their concentration was monitored by resonant one-photon laser-induced fluorescence (LIF) using ($2s^22p3s\ ^3P_J$–$2s^22p^2\ ^3P_J$) transitions near 166 nm. Pulses of vacuum-ultraviolet (VUV) laser radiation were generated using four-wave resonant difference frequency mixing in Xe [14,19]. LIF spectra confirmed that spin–orbit relaxation within the electronic ground state was achieved on a time-scale which was short relative to that for reaction [14]. For kinetic measurements, the VUV probe laser was tuned to the ($2s^22p3s\ ^3P_1$–$2s^22p^2\ ^3P_0$) transition at 165.69 nm and LIF signals were recorded at different time delays between the pulses from the photolysis and probe lasers. The recorded traces of LIF signal versus time accurately fitted single exponential decays yielding pseudo-first-order rate coefficients (k_{1st}). Second-order rate coefficients for reaction at a particular temperature were obtained from the slope of the linear plot of k_{1st} versus the concentrations of the C_3H_4 co-reagent.

2.2. Crossed beam experiments

The integral cross-sections for production of H atoms have been measured in the Bordeaux crossed molecular beam apparatus. Details of this machine have also been given elsewhere [20]. In the present experiments, $C(^3P_J)$ atoms were produced by laser ablation from a graphite rod and entrained into the supersonically expanded carrier gas (Ar, Ne or He), which originated from a first pulsed nozzle. This $C(^3P_J)$ atom beam crossed a pulsed C_3H_4 beam at an intersection angle which

Table 1
CRESU experimental conditions and rate coefficients for the reactions of $C(^3P_J)$ atoms with $CH_3C{\equiv}CH$ and $H_2C{=}C{=}CH_2$

Temperature (K)	15	27	54	83	207	295
Carrier gas	He	He	Ar	N_2	N_2	Ar
$[^3P_0]/[^3P_1]/[^3P_2]$[a]	0.59/0.36/0.05	0.36/0.46/0.18	0.22/0.43/0.35	0.18/0.40/0.42	0.14/0.36/0.50	0.13/0.35/0.52
Total density (10^{16} molecule cm^{-3})	5.05	4.65	5.36	4.88	5.83	19
Range of reagent gas (10^{14} molecule cm^{-3})						
$CH_3C{\equiv}CH$	0–0.82	0–3.5	0–4.2	0–3.7	0–4.8	0–50.8
$H_2C{=}C{=}CH_2$	0–1.9	0–4.0	0–4.9	1.1–3.8.	0–4.9	0–23.6
Rate coefficient (10^{-10} cm^3 $molecule^{-1}$ s^{-1})						
$CH_3C{\equiv}CH$	3.88 ± 1.62[b]	3.59 ± 0.32	2.43 ± 0.33	3.62 ± 0.45	3.10 ± 0.16	2.49 ± 0.20
$H_2C{=}C{=}CH_2$	2.91 ± 058	4.10 ± 0.55	3.42 ± 0.39	4.67 ± 0.60	3.63 ± 0.36	3.22 ± 0.32

[a] $C(^3P_J)$ spin–orbit populations.
[b] All error limits quoted are $\pm t\sigma$ statistical error where t is the appropriate value of student's t-distribution for the 95% point.

could be varied between 22.5° and 90°, allowing the relative translational energy for both reactions to be scanned over a wide range. Relative translational energies extending from ca. 4.9 to 284 meV could be accessed with the beam conditions listed in Table 2.

$C(^3P_J)$ atoms were detected, as described previously, using a two-photon LIF scheme [17,21]. The $H(^2S_{1/2})$ atoms produced in reactions (1) and (2) were probed in the beam crossing region by one-photon resonant LIF using the $(^2P_J–^2S_{1/2})$ Lyman-α transition at 121.57 nm. The VUV photons were generated by frequency tripling UV radiation around 365 nm in Kr [22]. Incident pulses (5 mJ, 6 ns) were focused with a movable fused silica lens ($f = 100$ mm) into a 170 mm long cell filled with ca. 10^4 Pa of Kr gas. Combination of this lens with a fixed MgF_2 lens ($f = 130$ mm at 120 nm), which also acted as an exit window, provided the desired collimation of the VUV radiation. The cell was set at the entrance of a light baffle arm, 1 m from the collision centre: the large difference in refractive index of MgF_2 between the VUV and the UV ensured elimination of most of the diverging incident UV radiation. The VUV beam propagated perpendicular to the molecular beam scattering plane, hence always perpendicular to the relative velocity vector of reagents.

In a typical experimental run, a batch of 25 LIF intensity measurements, each one being obtained by signal averaging over 16 laser pulses, was acquired at six different intersection angles between $\theta = 90°$ and 22.5°. Each run was repeated eight times, allowing the statistical uncertainties to be determined at 95% confidence interval assuming a atudent's t-distribution. This procedure ensured a short duration for a run (<7 min), thence avoiding any drift in the experimental conditions.

3. Results

3.1. Rate coefficients

The rate coefficients for the reactions of $C(^3P_J)$ atoms with the unsaturated hydrocarbons methylacetylene and allene are displayed as log–log plots versus temperature in Figs. 1 and 2. In each case, the variation of $k(T)$ with T is slight and the rate coefficients at all temperatures are close to the collision-determined limit. The data are fitted to the form $k(T) = A(T/298)^n$. The resulting thermal rate coefficients are $(2.7 \pm 0.6) \times 10^{-10}(T/298\text{K})^{-(0.11\pm0.07)}$ and $(3.5 \pm 0.8) \times 10^{-10}(T/298\ \text{K})^{-(0.01\pm0.12)}$ cm^3 molecule^{-1} s^{-1} for methylacetylene and allene, respectively. Only statistical errors

Table 2
Characteristics of the beams

Gas mixture	v (m s^{-1})[a]	$\Delta v/v$[b]	Δt (μs)[c]	$[^3P_0]/[^3P_1]/[^3P_2]$[d]
C-atom beam				
#1 Ar	810	0.07	13	0.42/0.43/0.15
#2 Ne	1070	0.09	10	0.39/0.46/0.15
#3 He	2210	0.09	6	0.39/0.46/0.15
$CH_3C{\equiv}CH$ beam				
#4 neat C_3H_4	830	<0.08	n.m.[e]	
#5 C_3H_4:0.33/He:0.67	1020	<0.08	n.m.	
$H_2C{=}C{=}CH_2$ beam				
#6 neat C_3H_4	830	< 0.08	n.m.	
#7 C_3H_4:0.33/He:0.67	1010	<0.08	n.m.	

[a] Velocity at the peak, uncertainty on v determination is ± 2%.
[b] Velocity spread half-width at 1/e (HWE).
[c] Pulse width (HWE) at the crossing point
[d] $C(^3P_J)$ spin–orbit populations.
[e] Not measured.

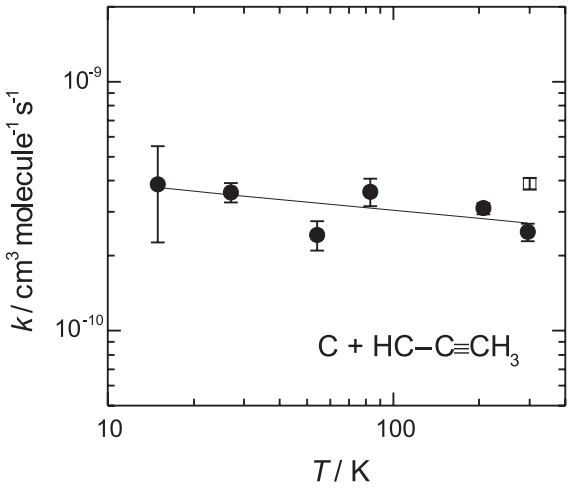

Fig. 1. Rate coefficients of the $C + CH_3C{\equiv}CH$ reaction. Symbols: filled squares, present results; open square, room temperature data (Ref. [1]); solid line, fit with $n = -0.11$ (see text).

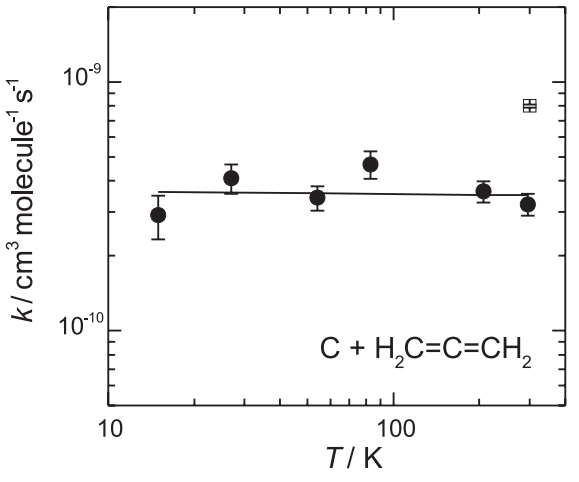

Fig. 2. Rate coefficients of the $C + H_2C{=}C{=}CH_2$ reaction. Symbols: filled squares, present results; open square, room temperature data (Ref. [23]); solid line, fit with $n = -0.01$ (see text).

(95% confidence level) are quoted. Some systematic errors may have arisen from, for example, inaccuracies in the calibration of flow controllers or in the determination of the total gas density, but it was estimated that these additional errors are no more than 10%.

The rate coefficients obtained in earlier studies at room temperature by Husain and coworkers [1,23] are also displayed in Figs. 1 and 2. Our value at room temperature is in fair agreement for $C(^3P_J)$ + methylacetylene, but a factor 2 smaller for $C(^3P_J)$ + allene.

3.2. Integral reaction cross-sections

Relative cross-sections have been measured as a function of relative translational energy for the production of hydrogen atoms in reactions (1) and (2). Several sources of background were present in these experiments: (i) dissociation of residual H_2O vapour in the chamber yielding OH + H and subsequent detection of the departing H atom, (ii) detection of cold H atoms present as an impurity in the C-atom beam, (iii) dissociation of the C_3H_4 beam in C_3H_3 + H with the same consequence as (i).

The first background signal was removed by shot-to-shot subtraction when triggering the Lyman-α laser beam at 10 Hz and the pulsed nozzles generating the C and C_3H_4 beams at 5 Hz.

The second background signal became negligible when tuning the laser off the centre of the transition. Indeed, these H atoms originating from the ablation process were strongly cooled in the supersonic expansion of the carrier gas. Therefore, they exhibited a Doppler profile limited by the bandwidth of the Lyman-α laser beam, $\Delta\nu = 0.6\ \text{cm}^{-1}$ half-width at 1/e (HWE), which was significantly narrower than the Doppler profiles, $\Delta\nu \approx 2\ \text{cm}^{-1}$ (HWE), resulting from the large translational energy release in these two very exoergic reactions. Three points are worth of note. Firstly, the reactive Doppler profiles are symmetric and unshifted relative to the centre of the transition ν_0, with widths given by the out-of-plane recoil velocity distribution of the H atoms, because the VUV beam propagates perpendicular to the scattering plane. Secondly, the fraction of H atoms observed when selecting a part in the Doppler profile is likely to remain almost constant when tuning the kinetic energy since the additional relative translational energy is much lower than the reaction energies. Thirdly, tuning the laser in the wing of the Doppler profile also eliminated possible contributions of reaction channels characterised by

a low reaction exoergicity, such as $C_4H_2 + H + H$ ($\Delta\varepsilon_0 > -0.2$ eV).

The last background signal (iii) was minimised by adjusting the collimation of the VUV laser beam, to avoid saturation of the Lyman-α transition. The remaining background from this source was then determined before each full experimental run by recording the signal with only the C_3H_4 beam switched on and was subsequently subtracted from the reactive signals. The problem arising from this background was more severe for methylacetylene than for allene because of its higher degree of photodissociation at 121.6 nm and because of lower reactive signal. It gave too low a signal-to-noise ratio with the beam combinations (beam #1 collided with beam #4) achieving the lowest kinetic energy. The data from C + methylacetylene were thus restricted to the 8.1–284 meV energy domain whereas the full 4.9–282 meV range could be considered for C + allene.

Relative values of the cross-sections were obtained by dividing the averaged signal intensities by the relative velocities of the reagents [24]. For each reaction, the resulting excitation functions (i.e., the variation of the cross-section with kinetic energy) obtained for different beam conditions gave distinct plots $\log\{\sigma\}$ as a function of $\log\{\varepsilon_{tr}\}$. All these plots were found to be well represented by $\log\{\sigma_i\} = \alpha_i \log\{\varepsilon_{tr}\} + C_i$ with almost the same slope α_i, allowing for normalisation when computing the rescaling factors C_i. With the same slope, α, taken as the mean value [20]. A final global fit on all rescaled curves yielded the normalised excitation functions displayed in Figs. 3 and 4.

Both cross-sections display a similar dependence on relative translational energy characteristic for a barrierless process: σ decreases monotonically with increasing kinetic energy. Fits of the experimental data yield $\alpha = -0.56 \pm 0.02$ and $\alpha = -0.55 \pm 0.01$ (95% confidence level) for methylacetylene and allene, respectively.

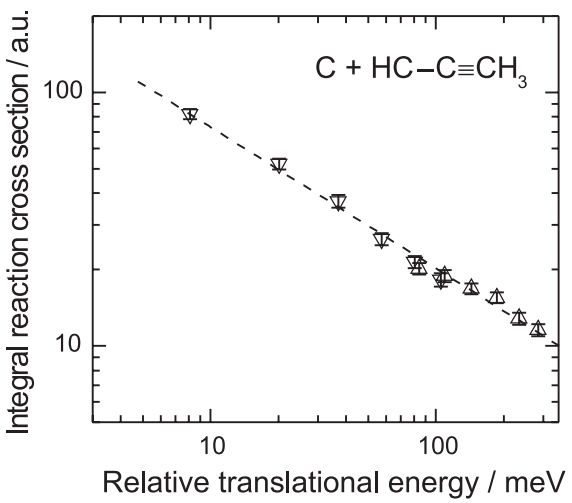

Fig. 3. Excitation function of the $C + CH_3C{\equiv}CH$ reaction. Experimental conditions: beam #2 collided with beam #5, down triangles; beam #3 collided with beam #5, up triangles; dashed line, fit with $\alpha = -0.56$ (see text).

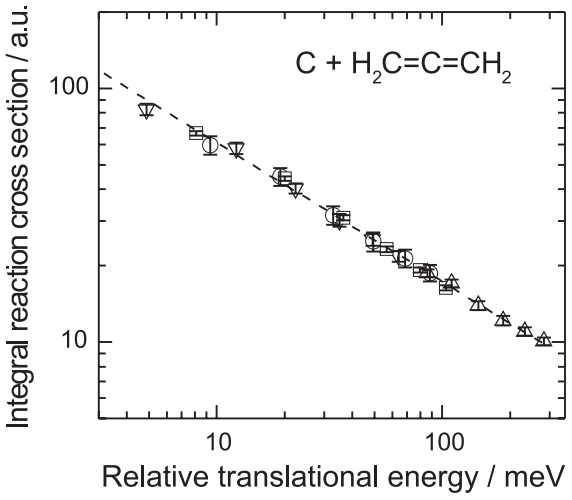

Fig. 4. Excitation function of the $C + H_2C{=}C{=}CH_2$ reaction. Experimental conditions: beam #1 collided with beam #6, down triangles; beam #2 collided with beam #7, squares; beam #2 collided with beam #6, circles; beam #3 collided with beam #7, up triangles; dashed line, fit with $\alpha = -0.55$ (see text).

4. Discussion

As discussed in previous papers, comparison between kinetics and dynamics results is based on the relationship between the excitation function and the thermal rate coefficient [15,20]. If the total reaction cross-section, σ_{reac}, is independent of the internal states of the reagents, the rate coefficient depends on the excitation function as follows:

$$k(T) = \left(\frac{8k_BT}{\pi\mu}\right)^{1/2} \int_0^\infty \sigma_{reac}(\varepsilon_{tr})(\varepsilon_{tr}/k_BT) \times \exp(-\varepsilon_{tr}/k_BT)\, d(\varepsilon_{tr}/k_BT), \quad (3)$$

where μ is the reduced mass of the reagents and k_B the Boltzmann constant. If it is assumed that the functional form $\sigma_{measured} \propto \{\varepsilon_{tr}\}^{\alpha}$ (in arbitrary units), determined in the crossed beam experiments, is representative of the total reaction cross-section, then integration is straightforward and yields $k(T) \propto T^n$, with $n = \alpha + 1/2$. This simple formula results in n values of -0.06 ± 0.02 for methylacetylene and -0.05 ± 0.01 for allene, values that compare very well with those obtained in the CRESU experiments (-0.11 ± 0.07 for methylacetylene and -0.01 ± 0.12 for allene).

Such an agreement is consistent with the assumption that $C(^3P_J)$ reactivity does not depend upon the spin–orbit state, J, involved, in so far as the two experiments are conducted with different relative J-populations: they are almost constant in the crossed beam experiments across the entire 4.9–284 meV energy range (see Table 2), whereas they vary strongly in the kinetic measurements between 295 and 15 K (see Table 1), since the J-levels are closely spaced with $J = 1$ (2) at 2.0 (5.4) meV above $J = 0$ and time is allowed for spin–orbit relaxation before starting the kinetic measurements. Furthermore, a significant spin–orbit effect on reactivity would result in a significant departure from the simple $k(T) \propto T^n$ functionality observed, which also justifies a posteriori the assumption made.

Whilst our kinetics measurements based on C-atom decay take account of all effective reactive channels among those energetically allowed [10,11], our crossed beam experiments based on H-atom detection are only sensitive to reaction pathways (1) or (2). Previous crossed beam experiments performed by Kaiser et al., at $\varepsilon_{tr} = 211$ and 344 meV for $C(^3P_J) + CH_3C{\equiv}CH$, $\varepsilon_{tr} = 203$ and 402 meV for $C(^3P_J) + H_2C{=}C{=}CH_2$, have identified the companion C_4H_3 fragment, detected on the $C_4H_3^+$ ion peak with a 'universal' mass detector rotating in the scattering plane, as the sole C_xH_y reaction product [10,11]. This finding along with our observation that the integral cross-sections increase monotonically with no sign of a threshold when energy decreases, indicate that reaction pathways (1) and (2) are likely to represent the dominant channels at lower kinetic energies, and hence at low temperatures.

Although the conclusion of Kaiser et al. [10,11], that the reactions of $C(^3P_J)$ atoms with methylacetylene and allene both produce $C_4H_3 + H$ exclusively is consistent with their quantum chemical calculations, it should be recalled that any reactive crossed beam experiment is subject to stringent signal-to-noise problems. Detectivity is at its best when the Newton sphere of the detected fragment is constrained around the centre of mass: the reaction flux is then analysed with the mass detector in a narrow range of laboratory angles. A good case is found when a heavy fragment recoils from an H atom, as is the case in reactions (1) and (2). In the case of the spin-forbidden insertion–elimination path leading to $C_4H_2 + H_2$, detectivity for the heavier product would become much lower because of the following effects, which both widen the range of laboratory angles over which the reaction flux is spread: first a larger reaction exoergicity ($\Delta\varepsilon_0 < -4$ eV), and second a less favourable partitioning of the recoil energy imposed by linear momentum conservation. Furthermore, a background $C_4H_2^+$ signal would arise from C_4H_3 fragmentation in the ioniser, within the range of laboratory angles where C_4H_3 recoils. Nevertheless, if several channels were present, the consistency of our kinetic and dynamical results would indicate that all channels involved exhibit a similar energy – hence temperature – dependence, emphasising that the reactions are governed by capture in the long range part of the potential.

In conclusion, this study unambiguously demonstrates that reactions of $C(^3P_J)$ atoms with both methylacetylene and allene are fast, even at very low temperatures, and that they proceed without any potential energy barrier on at least one reaction path, that leading to H-atom elimination.

Acknowledgements

The Birmingham group is grateful to EPSRC for a substantial research grant to construct their

CRESU apparatus, and to the EPSRC Laser Loan Pool at the Rutherford-Appleton laboratory which provided lasers. They also thank the EU (under its TMR programme) for a studentship (D.C.). The Bordeaux group acknowledges the support from the Conseil Régional d'Aquitaine and the Programme National Physique et Chimie du Milieu Interstellaire. Both groups are grateful for support of their collaboration *via* the provision by the EU of a TMR Research Network grant, contract FMRX-CT97-0132 (DG12-MIHT), for research on astrophysical chemistry.

References

[1] N. Haider, D. Husain, Z. Phys. Chem. 176 (1992) 133.
[2] N. Haider, D. Husain, J. Chem. Soc. Faraday Trans. 89 (1993) 7.
[3] N. Haider, D. Husain, J. Photochem. Photobiol. A 70 (1993) 119.
[4] D.C. Clary, N. Haider, D. Husain, M. Kabir, Astrophys. J. 422 (1994) 416.
[5] T.G. Phillips, P.J. Huggins, Astrophys. J. 251 (1981) 533.
[6] P. Shilke, J. Keene, J. Le Bourlot, G. Pineau des Forêts, E. Roueff, Astron. Astrophys. 294 (1995) L17.
[7] E. Herbst, Annu. Rev. Phys. Chem. 46 (1995) 27.
[8] R.P.A. Bettens, E. Herbst, Astrophys. J. 478 (1997) 585.
[9] R.I. Kaiser, D. Stranges, Y.T. Lee, A.G. Suits, Astrophys. J. 477 (1997) 982.
[10] R.I. Kaiser, D. Stranges, Y.T. Lee, A.G. Suits, J. Chem. Phys. 105 (1996) 8721.
[11] R.I. Kaiser, A.M. Mebel, A.H.H. Chang, S.H. Lin, Y.T. Lee, J. Chem. Phys. 110 (1999) 10330.
[12] I.R. Sims, J.L. Queffelec, A. Defrance, C. Rebrion-Rowe, D. Travers, P. Bocherel, B.R. Rowe, I.W.M. Smith, J. Chem. Phys. 100 (1994) 4229.
[13] D. Chastaing, P.L. James, I.R. Sims, I.W.M. Smith, Phys. Chem. Chem. Phys. 1 (1999) 2247.
[14] D. Chastaing, S.D. Le Picard, I.R. Sims, J. Chem. Phys. 112 (2000) 8466.
[15] W.D. Geppert, D. Reignier, T. Stoecklin, C. Naulin, M. Costes, D. Chastaing, S.D. Le Picard, I.R. Sims, I.W.M. Smith, Phys. Chem. Chem. Phys. 2 (2000) 2873.
[16] D. Chastaing, S.D. Le Picard, I.R. Sims, I.W.M. Smith, Astron. Astrophys., accepted.
[17] M. Costes, C. Naulin, C.R. Acad. Sci. Paris, Série II c, 1998, 771.
[18] P.L. James, I.R. Sims, I.W.M. Smith, M.H. Alexander, M.B. Yang, J. Chem. Phys. 109 (1998) 3882.
[19] R. Wallenstein, Optics Commun. 33 (1980) 119.
[20] C. Naulin, M. Costes, Chem. Phys. Lett. 310 (1999) 231.
[21] M.R. Scholefield, S. Goyal, J.H. Choi, H. Reisler, J. Phys. Chem. 99 (1995) 14605.
[22] R. Hilbig, R. Wallenstein, IEEE J. Quantum Electron. 12 (1981) 1566.
[23] D. Husain, A.X. Ioannou, J. Chem. Soc. Faraday Trans. 93 (1997) 3625.
[24] R. Vetter, C. Naulin, M. Costes, Phys. Chem. Chem. Phys. 2 (2000) 643.